

# UPGRADE OF DRAMA'S SPACECRAFT ENTRY SURVIVAL ANALYSIS CODES

**Ronny Kanzler<sup>(1)</sup>, Tobias Lips<sup>(1)</sup>, Bent Fritsche<sup>(1)</sup>, Davide Bonetti<sup>(2)</sup>, Irene Pontijas Fuentes<sup>(2)</sup>, Federico Letterio<sup>(2)</sup>, Gonzalo Vicario de Miguel<sup>(2)</sup>, Gonzalo Blanco Arnao<sup>(2)</sup>, Pedro Palomo<sup>(2)</sup>, Cristina Parigini<sup>(2)</sup>, Karl-Dietrich Bunte<sup>(3)</sup>, Anatoli Miller<sup>(3)</sup>, Christoph Garms<sup>(3)</sup>, Christopher Kebschull<sup>(4)</sup>, Stijn Lemmens<sup>(5)</sup>**

<sup>(1)</sup> *Hyperschall Technologie Göttingen GmbH, Albert-Einstein-Str. 11, 37191 Katlenburg-Lindau, GERMANY*

*Email: r.kanzler@htg-hst.de, t.lips@htg-hst.de, b.fritsche@htg-hst.de*

<sup>(2)</sup> *DEIMOS Space S.L.U., Ronda de Poniente, 19. Edificio Fiteni VI, portal 2, 28760 Tres Cantos (Madrid), Spain*

*Email: davide.bonetti@deimos-space.com, irene.pontijas@deimos-space.com, federico.letterio@deimos-space.com, gonzalo.vicario@deimos-space.com, gonzalo.blanco@deimos-space.com, pedro.palomo@deimos-space.com, cristina.parigini@deimos-space.com*

<sup>(3)</sup> *etamax space GmbH, Frankfurter Str. 3D, 38122 Braunschweig, Germany*

*Email: k.bunte@etamax.de, a.miller@etamax.de, c.garms@etamax.de*

<sup>(4)</sup> *Institute of Space Systems - TU Braunschweig Hermann-Blenk-Str. 23, 38108 Braunschweig, Germany*

*Email: c.kebschull@tu-braunschweig.de*

<sup>(5)</sup> *ESA/European Space Operations Centre, Robert-Bosch-Straße 5, 64293 Darmstadt, Germany*

*Email: Stijn.Lemmens@esa.int*

## ABSTRACT

Recently, ESA's Debris Risk Assessment and Mitigation Analysis (DRAMA) suite has been updated by implementing up-to-date methods and extending the functionality of DRAMA's Survival And Risk Analysis (SARA) codes, including the SESAM (Spacecraft Entry Survival Analysis Module) and SERAM (Spacecraft Entry Risk Analysis Module) submodules, which support the analysis of controlled and uncontrolled re-entries from LEO up to HEO regions, as well as objects returning from interplanetary space.

This paper provides an overview on the upgrade of the particular components, which include the handling of the aero-thermal and aero-dynamical modelling of the break-up and, moreover, the on-ground population forecast methodology. The extended capabilities, three-dimensional modelling of the spacecraft, including nested and connected break-up events and a CFRP ablation model, are described and the implementation with the existing DRAMA software is presented. To assess the potential transition from deterministic re-entry risk evaluation to a statistical one, a Monte-Carlo wrapper was implemented.

## 1 INTRODUCTION

Spacecraft re-entering the Earth's atmosphere after the end of their mission pose a potential risk for human life on-ground. Apart from global cooperation of the spacefaring nations, agreeing on common figures for the maximum risk acceptable, national or multinational space agencies have defined their own set of regulations about the details of the risk assessment and compliance verification rules for the re-entry of spacecraft built within the frame of a contract, or which are launched by a member state on its behalf.

The European Space Agency (ESA) has updated its own rules for space debris mitigation on March 28, 2014 (ESA/ADMIN/IPOL(2014)2), not only considering the re-entry but all mission-related items. The "ESA Space Debris Mitigation Compliance Verification Guidelines" [1], is now the guideline for all ESA-mission related debris topics for projects needing to demonstrate compliance to the requirements.

According to these regulations, the re-entry of a spacecraft has to be simulated with an ESA-approved software before it can be launched. In the early phase of the project, a positive (compliant) outcome has to be proved by an analysis with an ESA-approved object-oriented tool, while in later phases a spacecraft-oriented tool might need to be applied. For the provided codes to be meaningful as a compliance tool, they have to be validated and/or to be state-of-the-art. While there are different tools available, at least one in every state interested or involved in spacecraft launch, the ESA tools available for the early and later phases are DRAMA and SCARAB (Spacecraft Atmospheric Re-Entry and Aerothermal Break-Up).

The goal of the study, funded under ESA Contract No. 4000115057/D/SR, is the update of the re-entry and risk assessment modules (SESAM, SERAM) of DRAMA. SESAM, described in section 2, computes the re-entry history of the spacecraft, whereas SERAM (section 3) calculates the risk to the ground population. The modules are now accompanied by a Monte-Carlo wrapper (see section 4) to allow for statistical analysis. The implementation of the newly developed software modules into the DRAMA GUI is described in section 5.

At the time of writing of this paper, the study is in its final phase of validation and verification testing.

## 2 SESAM

In this section the upgrades carried out under DEIMOS Space responsibility in one of the two SARA modules, the Spacecraft Entry Survival Analysis Module (SESAM) which “simulates the controlled or uncontrolled re-entries of spacecraft into the atmosphere and calculates the survivability of spacecraft fragments”, are described.

Modelling the destruction of a re-entering object is a complex and highly stochastic multi-disciplinary problem. The dynamics of the entry must be coupled with the aerothermodynamics and the thermo-mechanical loads evaluation to fully model melting, deformation and fragmentation processes. Together with the detailed modelling of these processes, the object properties in terms of geometry, mass distribution and materials, are also required. In this frame, uncertainties play a significant role to cover both modelling approximation and unknown aspects (e.g. object geometric, mechanical and aerothermodynamical properties, atmospheric properties, entry conditions, etc.); in order to deal with them, Monte Carlo simulation capabilities are now available in SARA (see section 4 for further details).

### 2.1 SESAM architecture

Fig. 1 shows a high-level system context of the upgraded SESAM module, which clearly defines the three main areas of aerothermodynamics, dynamics and environmental models.

SESAM module has been entirely re-engineered, using an object-oriented programming paradigm and using the C++ programming language, see Fig. 2. This choice brings several benefits, in terms of tool maintainability and extensibility, along with a clear coupling between the object-oriented programming paradigm and physical spacecraft model. It allows a more generic handling of the relationships among objects composing a spacecraft (or a fragment of a spacecraft), their shapes properties,

their relative positions and attitude, their material properties and so on. The new SESAM architecture is now more structured and flexible, simplifying future tool improvements.

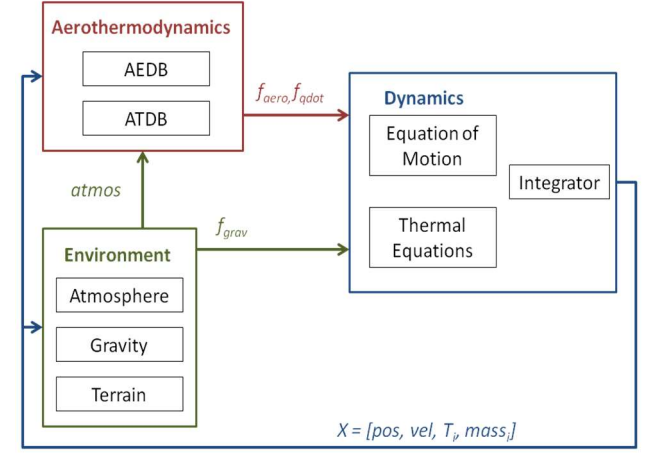


Figure 1. SESAM High-level System Context

### 2.2 SESAM functionality

The upgraded SESAM module keeps the object oriented approach but extending the currently available functionalities and including state-of-the-art features and innovative functionalities. Now SESAM is flexible enough to allow the users to define, for instance, different break-up triggers or re-entry attitude motions as well as to plug-in their own environmental or aerothermodynamics models (using those that best fit their needs) in order to cover a wider range of re-entry scenarios than before. The table below provides a comparison between the former and the upgraded SESAM module functionalities.

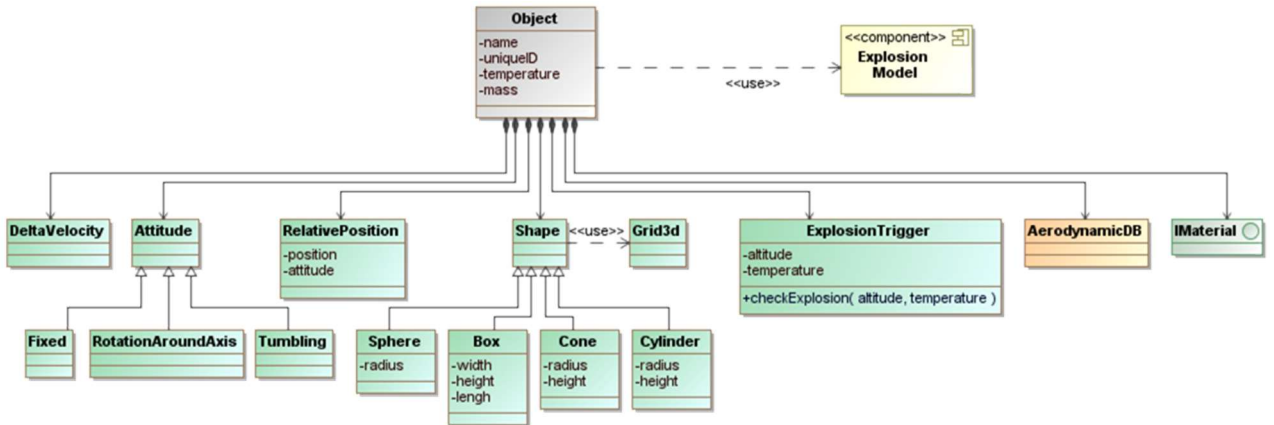
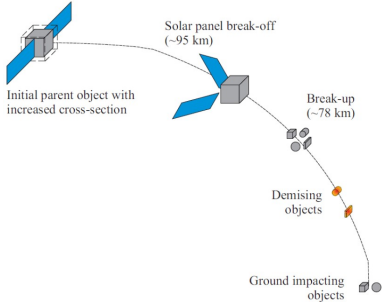


Figure 2. SESAM Object Class Diagram

Former SESAM functionalities	Upgraded SESAM functionalities
The software has been developed in <b>Fortran</b> .	The software has been developed in <b>C++</b> .
The <b>spacecraft is modelled on one single level of parent and child concept</b> : initially the spacecraft is modelled as a single simple object (e.g. a box of rough dimensions and total mass) which virtually contains all the other spacecraft components, without presenting any type of relationship between them.	The <b>spacecraft</b> (or the spacecraft fragment) <b>is modelled as a combination of multiple primitives</b> with two types of relationships between them: “ <b>included in</b> ” (one primitive is fully shielded by another one as in the parent/child concept) or “ <b>connected to</b> ” (two primitives are both partially exposed to the flow field and share a thermal conductive area). See [6].
<p>A <b>single spacecraft break-up event</b> is modelled. All the fragments are released at a pre-defined <b>fixed break-up altitude</b> (78 km). Solar panel break-off is possible and is set at 95 km.</p>  <p><i>Figure 3. Former SESAM breakup model [7]</i></p>	<p><b>Spacecraft fragmentation</b> (division into multiple fragments) <b>is a process</b> (not a single event) which is the result of the evolution of the relationships established between the primitives (see [6]). The “included in” or the “connected to” relationships are broken based on the integrated time histories of the aerothermodynamics of the fragment model along the propagated trajectory (see [6]). When a relationship is broken, a list of fragments is generated.</p> <p>The <b>thermal criterion is the default trigger</b> for the spacecraft fragmentation, however, users can define specific breakup triggers for particular objects (at inclusion or connected-to level); whichever trigger limit is reached first (default or user-defined) triggers the break-up.</p> <p>The available <b>user-defined triggers</b> are: altitude, heat flux, dynamic pressure, load factor and temperature.</p>
Spacecraft components are based on a pre-defined object list of simple shaped primitives: <b>sphere, box, cylinder, flat plate</b> .	Spacecraft components are based on a pre-defined object list of simple shaped primitives: <b>cones, boxes, cylinders, spheres</b> .
During the re-entry analysis of the fragments, <b>each object is treated individually</b> and does not influence the motion of the others (for example shadowing).	During the re-entry analysis of the fragments composed by multiple connected primitives, the <b>influence of shadowing is taken into account</b> . The fraction of visible primitive is computed at each time step and is used as relative weight in the sum of the fragment aerothermodynamics properties. This is achieved combining fast aerothermodynamic predictions with innovative shading factors computations (fraction of visible primitives) based on <b>voxels techniques</b> from computer graphics (see 2.3).
Trajectories are propagated in <b>3 degree of freedom</b> in terms of altitude and downrange. The variable time step solver Runge-Kutta 4-5 method is used to integrate the dynamics.	Trajectories are propagated in <b>3 degree of freedom</b> of a point mass under a given attitude mode. The fixed time step solver Runge-Kutta 7-8 method is used to integrate the dynamics.
Concerning the environmental model, the <b>US Standard Atmosphere 1976</b> is used together with a two-harmonics gravity model. An atmosphere variability of $\pm 20\%$ in density can also be applied in case of surviving objects to know the dispersion of the impact location needed for the risk analysis.	Concerning the environmental model, default values are provided based on the <b>US Standard Atmosphere 1976</b> and the <b>Horizontal Wind Model 2014</b> . However, <b>user defined profiles</b> can be provided as function of the altitude. Atmosphere variability in density can also be applied in Monte Carlo campaigns. A two-harmonics gravity model is included.
A material database is included, considering typical space materials (AA7075, A316, TiAl6V4, Copper and Inconel) but also allowing the inclusion of user defined materials up to 15 new ones. <b>Thermal properties</b> are modelled as <b>temperature independent</b> .	A material database is included, considering typical space materials. The tool also allows the inclusion of user defined materials (not limited to 15 new ones); <b>thermal properties</b> can be modelled as <b>temperature dependent</b> (e.g. emissivity, specific heat capacity and heat conductivity).
Aero-/Aerothermodynamic models are available for common simple geometrical shapes that are sphere, cylinder, flat plane or box.	<b>Aero-/Aerothermodynamic</b> models are available for common simple geometrical shapes that are sphere, cylinder, box or cone based on <b>pre-computed values</b> using DEIMOS in-house tools ( <b>HYDRA</b> and <b>HADES</b> modules from <b>PETbox</b> [5]) including dependencies on the flow regime, based on [13], [14], [15]. If needed, <b>user defined databases</b> as function of Mach and Knudsen

Former SESAM functionalities	Upgraded SESAM functionalities
	number are allowed.
Only <b>randomly tumbling</b> objects are taken into account, being the most common motion for the debris; therefore <b>no lifting capability</b> is modelled.	Different attitude modes can be specified for the fragments: <b>randomly tumbling, tumbling around a given axis and fixed attitude</b> ; therefore <b>lifting capability</b> is included. See [6].  Moreover, once a fragment composed by several objects is broken, there are two possibilities for the new fragments generated: to inherit the attitude from the parent fragment or to assume randomly tumbling motion.
For each shape, a <b>drag coefficient</b> profile is assumed. During the hypersonic flight, it depends on Knudsen number to model Free Molecular Flow, Transition and Continuum regimes (values adopted from ORSAT 5.0). At Mach equal to 1, the drag coefficient is reduced by 50% to model the subsonic aerodynamics, which is important to determine the ground impact energy. In fact, fragments are assumed to impact ground at their terminal velocity.	For each fragment shape, <b>drag, lift and side force coefficients</b> are computed for each flight condition as a combination of the primitives composing the fragment. Fragments impact velocity is obtained from the trajectory propagation.
The heat transfer formulation is similar to that implemented in ORSAT, in which heat flux in continuum and free molecular flow are distinguished. A uniform, averaged and shape dependent heat flux on the surface is assumed to model the incoming surface heat for a tumbling fragment: this is done by considering an approximate equivalent curvature radius depending on the shape. Averaged heating coefficients are adopted from ORSAT 5.0. Lumped mass model.	A <b>thermal network</b> is built where each primitive is represented by a thermal node (lumped mass model). The time evolution of temperature in the primitives is the results of the incoming and outgoing heat fluxes in each node along the fragment trajectory. <b>Conduction</b> is considered in case of “connected to” relationships.
<b>Thermal analysis is fully decoupled from the dynamics.</b> When the temperature reaches the melting temperature, melted mass is estimated but it does not affect the mass and size of the object considered in trajectory propagation.	<b>Thermal analysis and dynamics are coupled</b> , therefore, mass losses are considered during the trajectory propagation of the fragments.
Only ablation of <b>metallic</b> materials (melting) is implemented.	The ablation modelling has been extended to <b>CFRP-like materials</b> : pyrolysis (the epoxy matrix is decomposed under the action of the incoming aerodynamic heat flux) and oxidation (when the epoxy component near the outer border of the wall has gone, the remaining “charred” carbon fibres start to burn, with the carbon being transformed from the solid state to gaseous carbon oxide) effects have been modelled based on [2].
	An <b>explosion model</b> (based on NASA’s EVOLVE 4.0 [3]) has been implemented to generate a list of new fragments following an explosion event. Regarding the explosion triggers, there are two possibilities available, either based on altitude or based on temperature.

### 2.3 SESAM fragments modelling

The connected-to relationship introduced in the upgraded version of SESAM implies the possibility of having fragments whose external shape is not a simple primitive geometry. This feature adds a lot of flexibility in the spacecraft modelling to deal with more complex spacecraft definitions but also introduces new complexity and challenges not found in any previous object-oriented tool.

Solving the aerothermodynamics of a generic fragment

shape (any combination of multiple primitives) flying at any attitude and in any flight regime (from free molecular flow to subsonic) is not an easy task. In order to keep the computation reasonably fast, the approach followed in the upgraded SESAM is a linear combination of pre-computed free-stream primitives aerothermodynamic databases (alternatively, the user can set its own databases). The weights of this linear combination correspond to the fractions of visible surface of each primitive (if a primitive is fully shaded, its “visibility factor” is zero and it doesn’t contribute to the fragment’s aerothermodynamics).

To compute these visibility factors a new module in the SESAM has been introduced. As a first step, the fragment is modelled as a combination of small 3D cubes. This allows the creation of a 3D matrix of scalar values where zeros are set in the empty space and scalar values (1 to N) are assigned to the space filled by a given set of N primitive. In computer graphics, these are known as voxels (3D extension of the 2D pixels).

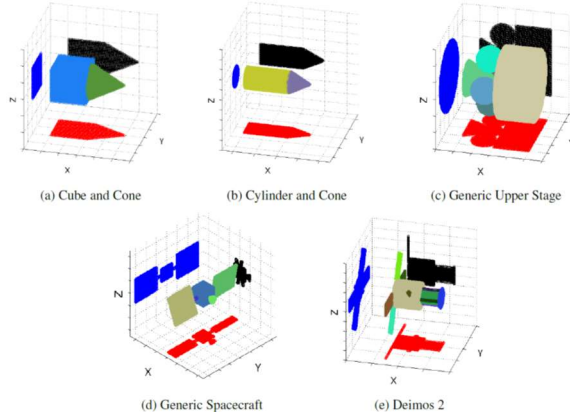


Figure 4. Examples of voxelized objects [4]

As a second step, for each fragment attitude, visibility factors for each primitive are computed as the ratio of the visible number of voxels in the scene associated to a given primitive to the total number of visible voxels if the primitive was placed in the domain by itself.

This new “**voxelator**” module of SESAM allows computing the visibility factors by manipulating a 3D matrix only (without the need for a more complicated ray-tracer module that needs appropriate surface meshes for each fragment). The compromise is that non linear effects are not captured (e.g. aerodynamic interactions of fragments made of multiple primitives).

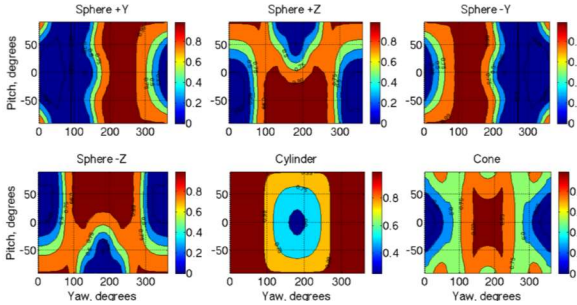


Figure 5. Examples of visibility factors for a Generic Upper Stage Model [4]

## 2.4 SESAM output

The main outputs provided by the upgraded SESAM module are

- Trajectory files for the re-entry initial body and its fragments in order to provide the time

evolution of their main thermal and trajectory parameters from the initial re-entry point down to their final conditions (demise, ballooning, skip-out or ground impact point).

- Final thermal state for the child fragments of the re-entry initial body (revealing which elements survive) and the ground dispersion, this information is used as an **input to the SERAM module** that run the risk casualty assessment (see section 3 for further details). Now, the cross-section at impact considering mass losses during the re-entry trajectory and floating capability over water/oceans are evaluated for the surviving fragments.
- Figures showing the altitude vs. time and altitude vs. downrange flown by all objects from the re-entry point down to their demise, ballooning, skip-out or impact point.

Fig. 6 and Fig. 7 show an example of the graphical output produced for an explosion event triggered at 100 km of altitude above ground. Up to 60 new fragments are generated, of which 18 are demised during the re-entry flight (blue plus-markers), 10 reach ground posing risk to human and 32 experience ballooning effect (red square-markers) being not considered risky since their kinetic energy is below the 15 J threshold.

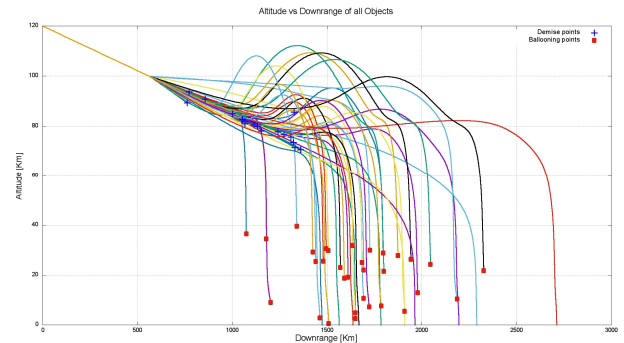


Figure 6. Example of altitude vs. downrange

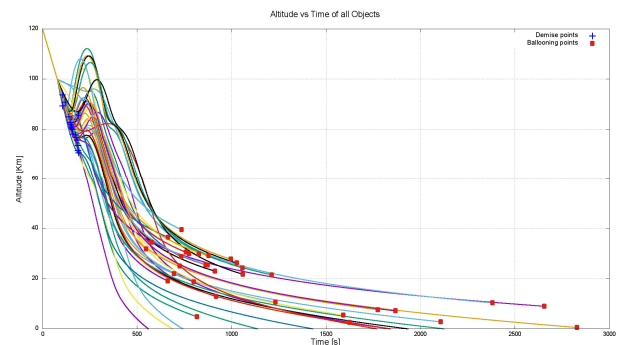


Figure 7. Example of altitude vs. time

### 3 SERAM

This section describes the upgrade of the SARA module SERAM (Spacecraft Entry Risk Analysis Module), which was upgraded under the responsibility of etamax space. SERAM performs the risk assessment of a given set of fragments impacting on ground and calculates casualty probabilities related to the fragments and the entire re-entry.

The module has been completely revised and newly coded. In addition a new population database has been integrated into the program. Two population data sources have been merged to allow future predictions of today's world population distribution. The population distribution of the world is derived from the Gridded Population of the World (GPW) and the future population predictions are deduced from the United Nations World Population Prospects (UNWPP) for eight different population growth scenarios. While in the original SERAM code, population growth has been taken into account by assuming exponential growth, now the future population evolution is determined until the year 2100 from country dependent population predictions provided by the UNWPP data.

The new SARA supports controlled and uncontrolled re-

entries from LEO and HEO regions. For this reason both two dimensional (latitude and longitude dependent) as well as one dimensional (only latitude dependent) population data is required for the risk analysis. In this section SERAM's new functionality will be presented and the preparation, handling and implementation of the population datasets into the SERAM module will be outlined.

#### 3.1 SERAM functionality

The new SERAM has been completely redesigned and the programming language changed from Fortran to JAVA.

Fig. 8 shows the workflow of the new SERAM. The module first reads the paths to all required input files (seram.xml), the re-entry scenario (sara.xml) and the list of the fragments that impact on ground (impactingFragments.xml). While the re-entry scenario is defined by the user, the list of the impacting fragments is calculated by SESAM (see section 2 for further information). In the new SARA, the list of impacting fragments can also be defined by the user, e.g. if the user only wants to analyse the risk related to a previously known list of fragments, e.g. generated by an analysis with a different tool.

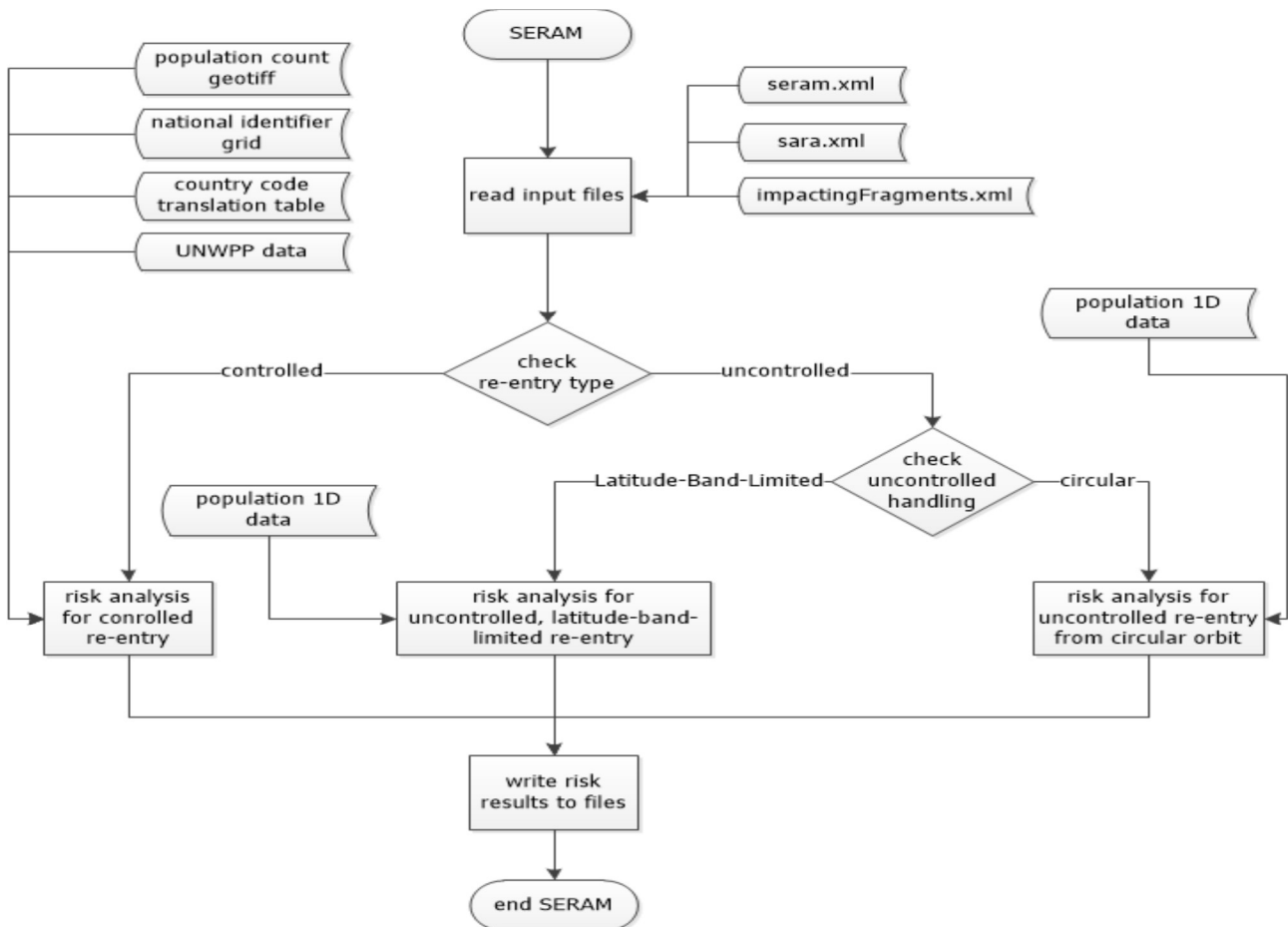


Figure 8. SERAM workflow



The impacting fragments list contains all fragment related data, which is required for the risk analysis:

- fragment ID
- impact epoch
- impact mass
- impact velocity
- impact location (latitude and longitude)
- fragment cross section at impact

The re-entry scenario data comprises the following data required for the risk analysis:

- re-entry type (controlled or uncontrolled)
- handling method for uncontrolled re-entries (i.e. re-entry from near circular orbit or latitude-band-limited re-entry)
- UNWPP population growth scenario
- impact energy limit of a fragment, where no casualty is to be expected
- orbit inclination (required for uncontrolled re-entry)

With the scenario and impacting fragments information the on ground risk arising from a re-entry event can be determined. The SERAM module distinguishes between controlled and uncontrolled re-entries. Controlled re-entries are re-entries, where the coordinates of the impact location are known whereas a spacecraft that re-enters in an uncontrolled manner can impact anywhere in the latitudinal range of its ground track.

Furthermore uncontrolled re-entries are sub-divided into re-entries from near circular orbits and latitude-band-limited re-entries. While re-entries from near circular orbits amongst others represent natural decays, latitude-band-limited re-entries reflect re-entries from highly elliptical orbits (HEOs), where re-entry is likely to occur in the proximity of the perigee [8]. Unfortunately, currently no theory is available for an analytical calculation of the risk related to re-entries from HEOs.

In the new SERAM the risk related to controlled and latitude-band-limited re-entries is only evaluated deterministically. The impact locations are read from the impactingFragments.xml file and risk is determined for this particular location. To derive statistical conclusions a Monte-Carlo Wrapper has been developed and implemented into the new SARA (see section 4 for further details).

Three main risk calculation classes are implemented into the new SERAM. While the risk for controlled and latitude-band-limited re-entries is determined only deterministically (fragment's impact probability  $P_i$  is set to  $P_i = 1$  at the impact location), an uncontrolled re-entry from a near circular orbit can be evaluated analytically. For this re-entry type the probability of an impact on a particular latitude is a function of the latitude  $\varphi$  and the orbit inclination  $i$ :

$$P_i(\varphi) = f(\varphi, i) \quad (1)$$

The theory of the risk assessment and calculation in the new SERAM is the same as in the older SERAM. The methodology has been described by Klinkrad in [9].

The risk (casualty probability  $P_c$ ) that arises from a set of fragments impacting on ground is a function of the three parameters impact probability  $P_i$ , population density  $\rho_P$  and the casualty area  $A_c$  of a fragment:

$$P_c = P_i \cdot \rho_P \cdot A_c \quad (2)$$

The casualty area is the area, where the fragment can hit a standing human person. As mentioned before in the new SERAM the local impact probability is either set to "1" (controlled and latitude-band-limited re-entry) or it is calculated depending on the latitude and the orbit inclination. The impact probability is predetermined by the user, due to the choice of the re-entry type, and the casualty area is derived from the fragment's impact cross section, which is provided by SESAM.

The population density at the impact location is the main element in SERAM. Depending on the user's input and re-entry type either 1D (only latitude dependent) data is required for the uncontrolled and latitude-band-limited risk analysis and 2D (latitude and longitude dependent) population data is required for the controlled risk analysis. The determination of the 1D and 2D population density, which serves as input for the casualty calculation, will be discussed in section 3.2.

As a new feature of the new SERAM, the calculation of the fatality probability has been implemented. While the casualty probability takes into account any direct hit of a person, the fatality probability differs, by only taking into account fragments that would be lethal. Fragments with kinetic impact energies  $E_{kin}$  up to a pre-defined kinetic energy limit  $E_{low}$  are considered to be non-lethal. Fragments with kinetic impact energies above an upper limit  $E_{high}$  would always be lethal. In between this range, a transition function is applied to assess the fatality probability:

$$P_f = \eta_f \cdot P_c \quad (3)$$

with

$$\eta_f = \begin{cases} 0 & \text{for } E_{kin} < E_{low} \\ \frac{1}{2} - \frac{1}{2} \cos\left(\pi \frac{\ln(E_{kin} [J]) - \ln(E_{low})}{\ln(E_{high}) - \ln(E_{low})}\right) & \\ 1 & \text{for } E_{kin} > E_{high} \end{cases} \quad (4)$$

### 3.2 Population Database

The population density at a particular location and time is derived from two data sources. The Gridded Population of the World (GPW) provides data of the areal distribution of the human population on the world for the reference year 2015. The GPW data is provided in a GeoTIFF file format. The GeoTIFF is a raster of the world, where each pixel contains a value representing e.g. the population count in this pixel. The borders of the pixel represent the northern and southern latitude and the western and eastern longitude, respectively. The GPW data used in the new SERAM is the GPW version 4 GeoTIFF, where each pixel has a resolution of 30'', which is approximately 1km x 1km at the equator [10]. Since the population data can only be provided for discrete pixels, the risk related to a fragment impacting on ground is also calculated for this corresponding area.

The second population data source is the United Nations World Population Prospects (UNWPP). These are provided in tabular format and contain country dependent as well as total world population counts for the years 1950 to 2100 in eight different population growth scenarios (see Fig. 9).

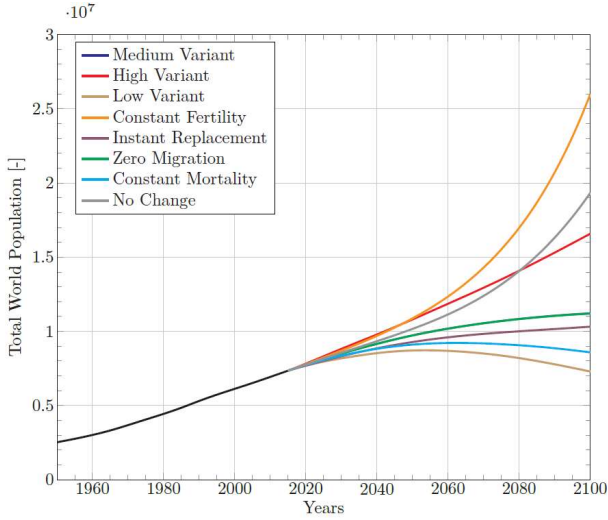


Figure 9. UNWPP population growth scenarios

Controlled re-entries require 2D population data, which is read from the GPW GeoTIFF. Since this world population distribution is only available for a certain reference year, population growth needs to be applied to estimate the population of the year of the re-entry. To allow a higher accuracy of the population evolution, this evolution is estimated on the basis of the country's population growth. A second GeoTIFF containing information about the country of any coordinate on the world is used to assign an impact location to a country. With the information of the population of the reference year, the country of the impact location and the UNWPP data for population growth, all data is available to determine the population density at a particular location

and in a particular re-entry year. The population growth rate of the country of the impact location is applied to the population density of the reference year to determine the required population density of the re-entry year at the impact location.

GPW also provides a GeoTIFF with each pixel containing information about the population density. According to the GPW documentation, this population density is only the density of the land area within this pixel [10]. Fig. 10 shows a cut-out of the land area of a Polynesian island, where a black pixel represents 100% land in this pixel and a white pixel represents 100% water. The different grey shades at coasts and small islands cause problems, because the actual population density of the entire pixel cannot be determined without further effort. Since the risk results in SERAM shall always represent the risk associated to a whole pixel, a different method is used to determine the population density of a pixel.

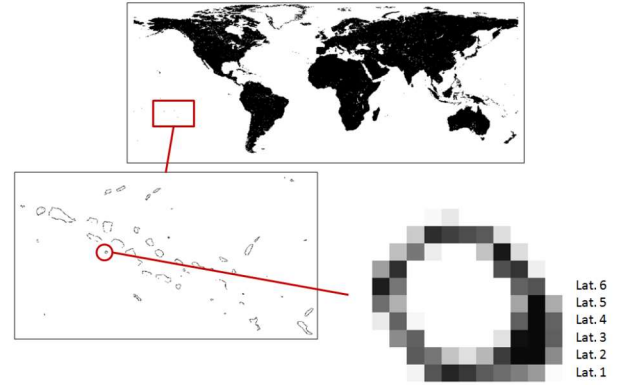


Figure 10. GPW land area GeoTIFF cut-out

Instead of the population density, the new SERAM uses the population count GeoTIFF provided by GPW. To determine the population density of each pixel, the area of a pixel needs to be calculated. Since the longitudes are converging from the equator to the poles, the area of a pixel varies as a function of the latitude. The latitudes are equidistant in the GeoTIFF. The area of a pixel is determined by calculating the area of a single latitude bin (see green area Fig. 11) and dividing this area by the number of pixels of this latitude bin. The latitude bin is the spherical segment of all pixels in a single latitude band.

$$A_{\text{pixel}} = \frac{A_{\text{bin}}}{n_{\text{pixel}}} \quad (5)$$

The area of the spherical segment is calculated from the latitudes of the upper and lower border of the pixel, where the fragment impacts (see Fig. 12). The area of the spherical segment is calculated from the latitudes of the upper and lower border of the pixel, where the fragment impacts (see Fig. 12). The equation of the spherical segment area assumes the Earth to be spherical. Since the



difference between the upper and the lower latitude is small, this simplification is acceptable. The mean Earth radius of the latitude bin  $R_m$  is the corresponding Earth radius of the average of the upper and lower latitude. It is calculated by taking into account the flattened Earth.

$$A_{bin} = 2 \cdot \pi \cdot R_m \cdot h_{bin} \quad (6)$$

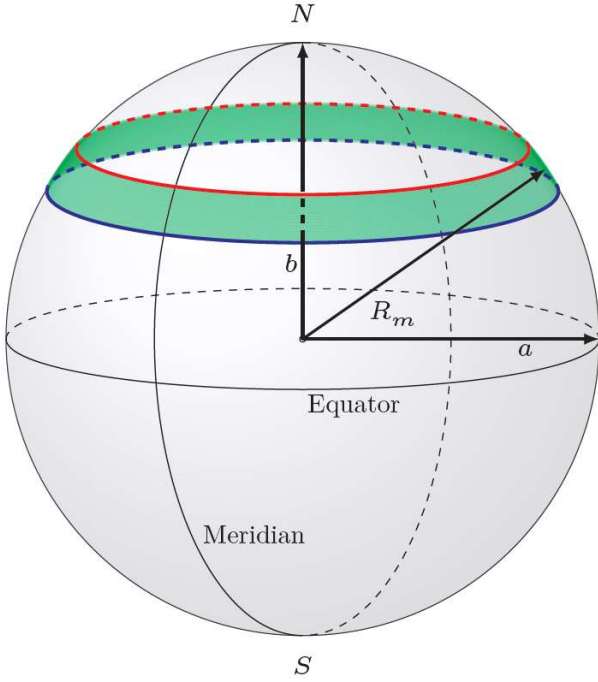


Figure 11. Latitude bin (green) on a simplified Earth

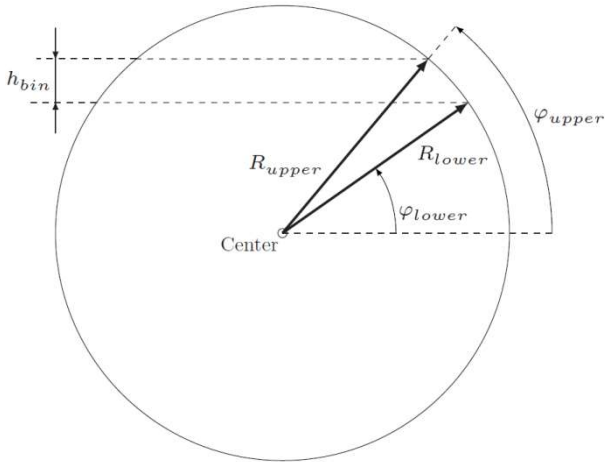


Figure 12. Latitude bin as section with parameters of the pixel area calculation

Finally, the population density of the pixel is the quotient of the population count (read from the GeoTIFF) and the calculated pixel area. In the risk calculation, this population density of the reference year is then adjusted

by applying a factor of the population growth between re-entry and reference year.

For uncontrolled re-entries (from near circular orbit and latitude-band-limited), 1D population data is required. This only latitude dependent data is the mean population density per latitude bin. The 1D population density per latitude is calculated from the total population count of the entire latitude bin, divided by the area of the spherical segment of the latitude bin. The total population count of the latitude bin is the sum over all longitudes  $\lambda$  between  $\lambda = -180^\circ$  and  $\lambda = +180^\circ$ .

$$\rho_P(\varphi) = \frac{\sum_{\lambda=-180^\circ}^{+180^\circ} c(\varphi, \lambda)}{A_{bin}} \quad (7)$$

To determine the latitude dependent population density of other years, this 1D population density of the reference year needs to be adjusted by an average population growth rate of the particular latitude bin. Since the UNWPP data provide country dependent population growth rates, the pixels of a latitude bin can be evaluated individually, by weighting the growth rate of the complete bin with the local population growth rates of the countries within this latitude bin. A separate population data preparation tool is provided, which calculates the 1D population densities for all years the UNWPP data comprises. Fig. 13 Shows the 1D population densities as applied in the new SERAM for one of the eight UNWPP population growth scenarios.

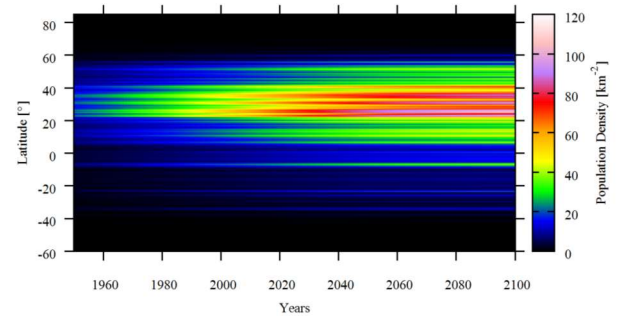


Figure 13. 1D population density for the years 1950 to 2100

The pre-calculated 1D population density data is used as input in SERAM, if a risk analysis shall be performed for an uncontrolled re-entry.

### 3.3 SERAM output

The output of the new SERAM comprises the casualty and fatality probability results for each impacting fragment as well as the total casualty and fatality probability related to the entire re-entry event. Depending on the re-entry type, 1D and 2D risk results are calculated and provided to the user. The output of a controlled re-entry is the 2D casualty and fatality results of the impact location as well as 1D casualty and fatality results, where

only the latitude of the impact location is considered and the 1D population density of this latitude bin is used in the casualty probability calculation. For uncontrolled and latitude-band-limited re-entries, only the 1D risk results are calculated from the 1D population density data. The risk results are summarized in a “RiskResults.xml” file together with the input and scenario setup of the risk analysis. Besides the summary in the risk results XML file, the casualty and fatality probability of each fragment and the entire re-entry event are also written to .DAT files, which are used by Gnuplot drivers.

The Gnuplot drivers create plots of the casualty, fatality and impact probability as a function of the latitude. Fig. 14 shows the casualty probability for an uncontrolled re-entry from a near circular orbit. The risk analysis has been performed for a satellite with 125 fragments impacting on ground.

Furthermore, for controlled re-entries also the impact locations are plotted. Fig. 15 shows the impact locations of a satellite re-entering from a sun-synchronous orbit.

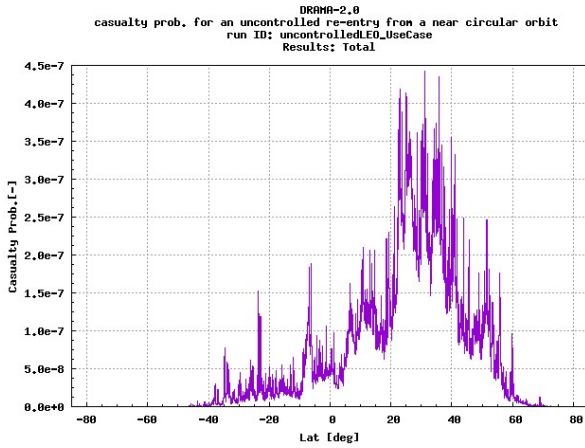


Figure 14. Casualty probability for an uncontrolled re-entry from a near circular orbit

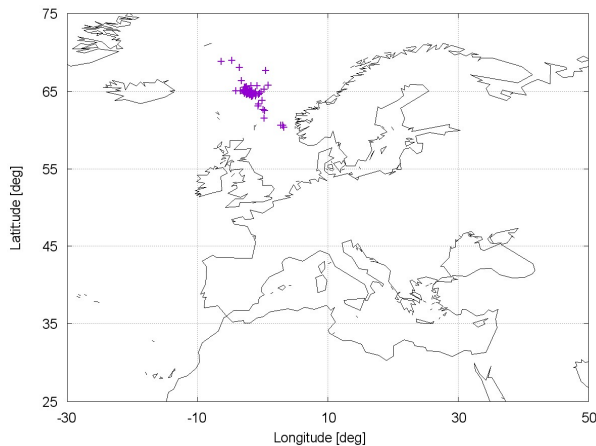


Figure 15. Impact locations for a controlled re-entry on a sun-synchronous orbit

## 4 MONTE-CARLO WRAPPER

The Monte-Carlo wrapper, developed by HTG, is a new module in the updated DRAMA, not present in previous versions. Its purpose is to provide DRAMA with the capability to perform a variational analysis for a given reference re-entry problem. For this purpose, the reference re-entry conditions are varied, and for each variation, SESAM and/or SERAM are called. Afterwards all simulations are evaluated.

### 4.1 Variation

Previous DRAMA versions were purely deterministic, i.e. all input data were defined as a unique set of data, and one simulation was performed for this data set. In the new DRAMA it is still possible to perform single simulations with SESAM and/or SERAM, but it is also possible to study the variation of the simulation results under a variation of the input data set. In general there are four types of variations possible:

#### Parametric variation

The reference variable is varied in fixed steps, starting at a lower limit and finishing at an upper limit.

#### Stochastic variation

In this case, a normal distribution is assumed for the variation, with the reference value as mean, and with the variance and number of samples specified.

#### Probability distribution

This case is similar to the previous one, but with an arbitrary probability distribution and number of samples specified.

#### Selection

Some input variables can have discrete values only, e.g. (on, off). This case can be handled with the selection type.

For the implementation, it is necessary to consider that there are also different types of variables:

#### Method-related parameters

These are the input parameters of SESAM and SERAM. Examples are the initial conditions for SESAM (e.g. position and velocity components) and scenarios for SERAM (controlled/uncontrolled).

#### Object-related parameters

These are the parameters describing the geometry of the re-entering spacecraft. Examples are dimensions and scaling factors.

#### Material parameters

These are the material properties. Examples are density, heat capacity, and emissivity.

It depends on the type of parameter which variation method makes sense to vary. Apart from this limitation, the variation concept is very versatile and many parameters could be varied in different ways. In practice, the DRAMA GUI restricts the variation possibilities to the meaningful ones.

## 4.2 Evaluation

The following simulation results are evaluated.

Ground dispersion:

- latitude and longitude ranges
- along-track and cross-track ranges
- bounding box, Declared Re-entry Area (DRA), Safety Re-entry Area (SRA)

Fragment-related risk data:

- impact location (latitude and longitude)
- 1D and 2D casualty probability
- 1D fatality and 2D fatality probability,
- mass
- casualty area

Total risk data:

- 1D and 2D casualty probability
- 1D and 2D fatality probability
- total impacting mass
- total casualty area

### 4.2.1 Ground Dispersion

The latitude and longitude ranges are found by enveloping all impact locations by a rectangular box. For the evaluation of the along-track and cross-track ranges the impact points locations are fitted by a third-order polynomial. Then for each impact point the cross-track distance to the fit curve is determined by finding the intersection point between the fit curve and a line through the impact point with direction normal to the fit curve. Numerical integration of the distance of the intersection point to the start of the fit curve gives the along-track distance.

The bounding box of the impact points is the enveloping rectangle of their along-track/cross-track distances. DRA and SRA are determined by shrinking the bounding box equally from its ends until the specified number of impact points are contained in this new box (99% for DRA, 99.999% for SRA).

The distribution of the impact points can be analyzed statistically. For this purpose the bounding box is discretized into a number of bins in along-track and cross-track direction.

### 4.2.2 Risk Data

Fragment-related risk data are of interest for a detailed analysis of the risk distribution. They are compiled from the SERAM runs and output into a single data file. For

plotting purposes GNUPlot driver files are generated.

The total risk data are compiled from the SERAM runs and output into a single data file as well, but additional statistical evaluations are performed. For this purpose the data distributions are discretized into a number of bins. The probability distribution as well as the cumulative probability are evaluated.

## 4.3 Example

In the following, the new approach is illustrated for a simple example. Only three SESAM input parameters were varied:

- Radius (stochastic, variance: 10 km, 5 samples)
- Velocity magnitude (stochastic, variance: 10 m/s, 5 samples)
- Flight path angle (parametric, from  $-3^\circ$  to  $-0.5^\circ$ , step size:  $0.5^\circ$ )

Together these are 150 variations (and therefore simulations). In all cases 3 fragments were reaching ground, so there are 450 impact points in total.

Fig. 16 shows the impact point locations and the fit curve. Actually, also the bounding box is plotted, but it is difficult to recognize, due to the very narrow spread of the impact points.

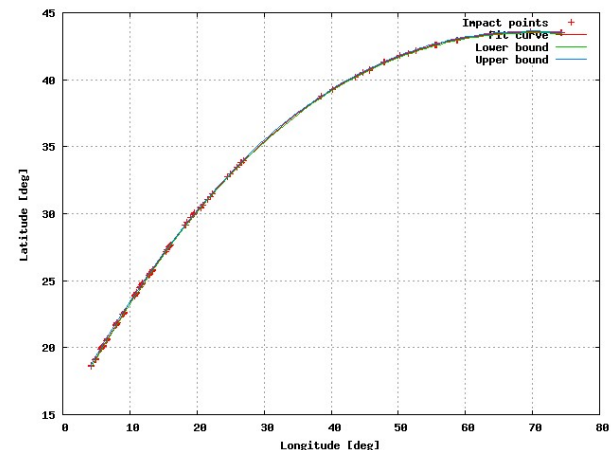


Figure 16. Impact point locations and fit curve

Fig. 17 shows the impact points with their along-track and cross track coordinates. The length of the ground track is about 7000 km, while the width is only  $\pm 7$  km.

Fig. 18 shows the 1D casualty probability for all fragments as function of latitude and Fig. 19 shows the same for the 2D casualty probability. The figures look quite different. The difference is due to the different definition of 1D and 2D casualty probability. The 2D casualty probability takes into account the local population density along the actual impact points. This density peaks at about  $40^\circ$  latitude, which corresponds to a longitude of  $45^\circ$ . At this location, the impacting fragments obviously hit by chance a densely populated

area. The 1D casualty probability is computed with the population density averaged over the whole latitude band. This density has maxima at about 22°-24°. This latitude band crosses China, India, and Mexico, for example.

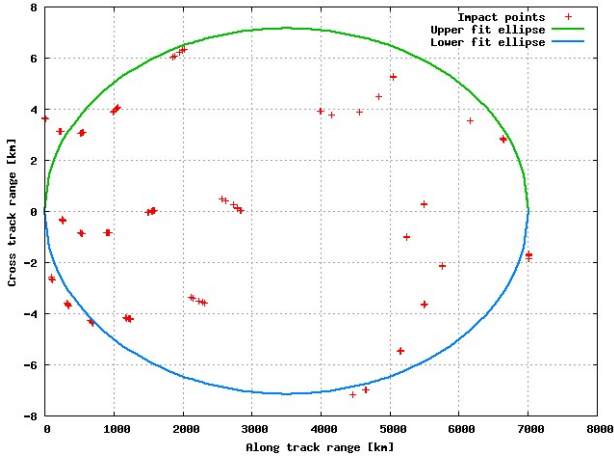


Figure 17. Along-track and cross-track coordinates of impact points

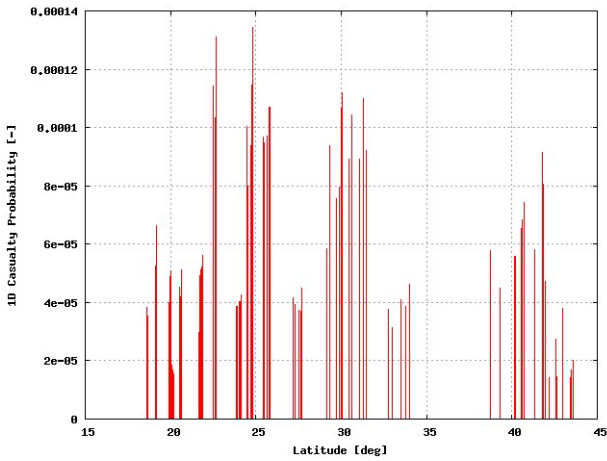


Figure 18. 1D casualty probability for all fragments

Fig. 20 shows the PDF of the total 1D casualty probability. Fig. 21 shows the corresponding cumulative PDF, i.e. the distribution shown in Fig. 20 integrated over the casualty probability. From this figure it can be stated, for example, that with about 70% confidence the casualty probability will be below  $2.2 \cdot 10^{-4}$ .

Again, it is interesting to compare with the 2D casualty probability. Fig. 22 shows its cumulative PDF. It shows, that for the actual impact points the 2D casualty probability is with 90% confidence below  $5 \cdot 10^{-5}$ !

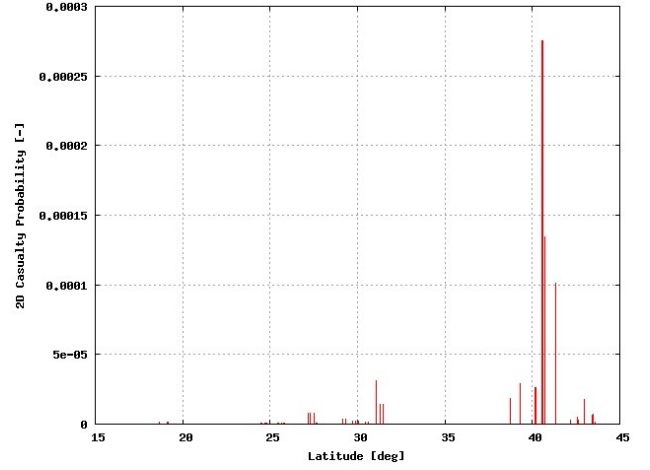


Figure 19. 2D casualty probability for all fragments

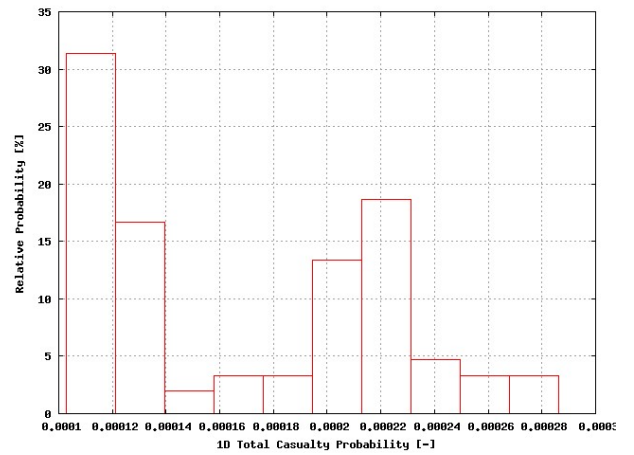


Figure 20. PDF of the total 1D casualty probability

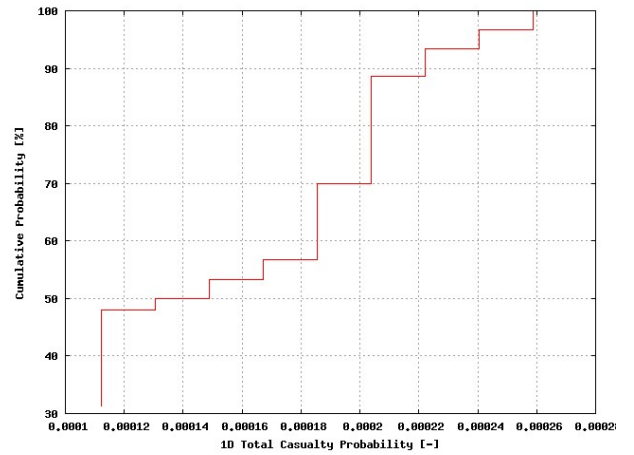


Figure 21. Cumulative PDF of the total 1D casualty probability



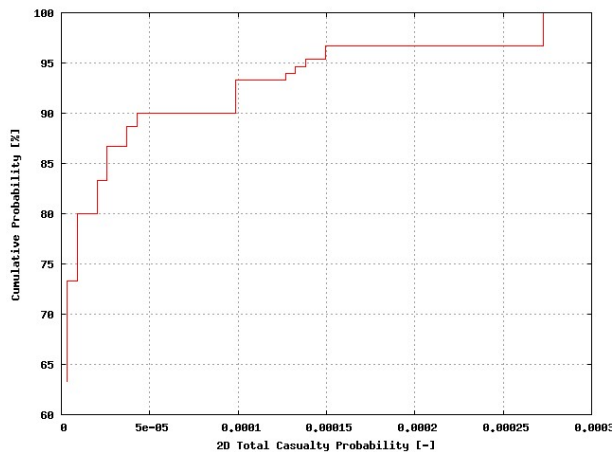


Figure 22. Cumulative PDF of the total 2D casualty probability

## 5 DRAMA GUI IMPLEMENTATION

The Graphical User Interface (GUI) has been updated to reflect the new functionality of SARA. The GUI is based on a Java framework developed at IRAS, which was developed for MASTER 2009 and PROOF 2009 [11]. It was later adapted for DRAMA 2.0 in order to provide a similar look and feel to the user [11]. It has been further enhanced for the upgrade to the SARA code for version 3.0 of DRAMA. In the following the changes to the GUI

are outlined. First the new definition of the satellite body is discussed, followed by an overview of the more complex sidebar, which now contains four main entries:

- Basic Settings
- Model
- Fragment Model
- Monte Carlo

Each sidebar entry is enabled and can be accessed in a given run and configuration mode of the SARA tool.

### 5.1 Object Modelling

Compared to the previous SARA version the most obvious change in the GUI is the shift from the flat hierarchy in the object modelling to an object-oriented approach. When modelling a spacecraft or rocket body the subsystems and components can be contained within one another. For easy access to the multiple layers of hierarchy a tree structure was chosen to visualize the satellites architecture as opposed to the table-based approach in DRAMA 2.0. Fig. 23 shows the new tree structure of the spacecraft. It is paired with a 3D representation of the selected component and all other components on the same hierarchical level. The selected component is highlighted using white colour in contrast to other components, which are displayed in grey. The components can be defined similar as in the CROC

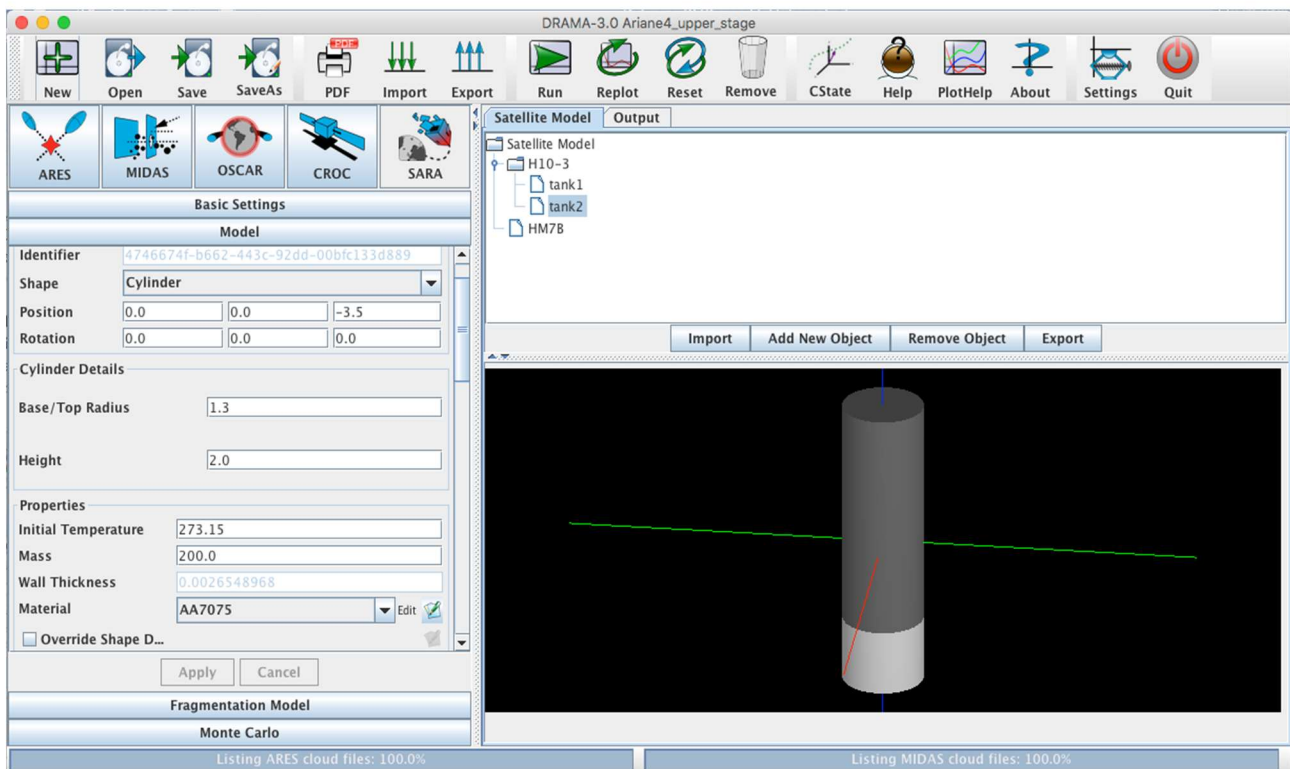


Figure 23. DRAMA GUI in the SARA view, showing the re-worked sidebar, the tree structure of the model, which allows the hierarchical definition of satellite systems. Below the tree structure is the graphical representation of the components hierarchical level.

module. Each component has a primitive shape (sphere, cylinder, cone or box). The dimensions and 3D positions can be defined. In addition, the material can be chosen: from either CFRP or metal material databases. Based on the selection of shape, dimension and materials the GUI calculates the wall thickness of the given structure and displays it. A new feature within this update is the ability to specify connected-to relations for components on the same hierarchical level. Based on these relations triggers can be defined: breakup and explosion triggers, as well as an override for specifying the imprinted delta-velocities after a triggered event occurs. DRAMA 3.0 brings the ability to import and export satellite subsystems and components. The GUI gives access to corresponding databases. Using the context menu in the Satellite Model or the Material databases also lets the user export the selected items to the filesystem. This enables a simple exchange of subsystems, components and materials, apart from the Import and Export options in the toolbar on top.

## 5.2 Sidebar

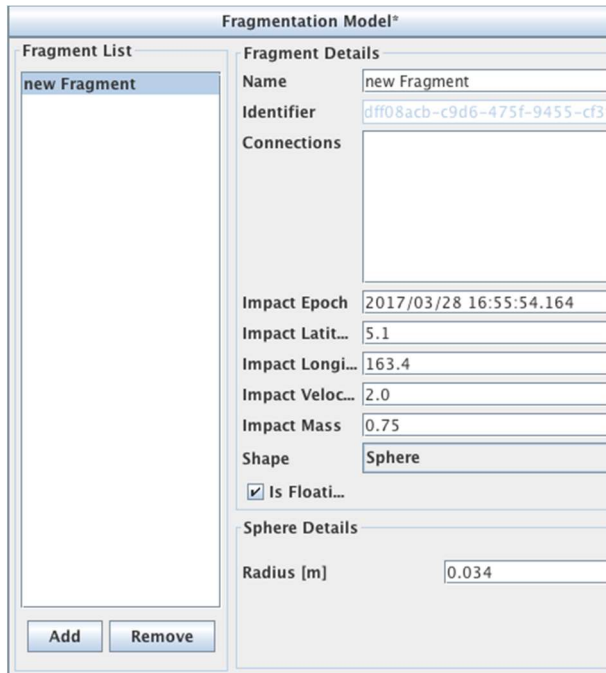


Figure 24. Fragmentation Model sidebar section.

The sidebar on the left can show up to four sections containing different settings for the categories as summarized in Table 1. The different configuration and run modes can be chosen in the Basic Settings. The experienced user can activate the *Expert Mode* in order to gain more control over the configuration of the simulation and the properties of the model. Furthermore, in *Expert Mode*, the simulation can be configured to run in either the *Re-entry-only*; *Risk-only* or *Re-entry + Risk* configuration. The configurations for the standalone

modes can be accomplished in the corresponding sidebar sections. An additional *Monte Carlo* mode can be activated.

Table 1: Overview of sidebar sections.

Section	Purpose	Default mode	Expert mode
Basic Settings	Define simulation details	X	X
Model	Define satellite model and its properties	X (partially)	X
Fragmentation Model	Define fragments and their properties	-	X
Monte Carlo	Define variations for inputs from the sections above to execute Monte Carlo runs and statistical analysis.	-	X

## 5.3 Fragment Modelling

For the re-entry analysis, the user has to specify a *Satellite Model*. It is then used by the SESAM tool to simulate the re-entry and breakup of the body into fragments. Fragments may reach the ground and pose risk to the population. These fragments are then handed over to the SERAM tool in order to perform a risk analysis. When the user wants to skip the computationally intensive re-entry and breakup simulation, he can choose to enable the *Risk-only* mode. In *Risk-only mode* the *Fragment Model* sidebar entry is available. The user can define the impacting fragments by hand and perform the risk analysis based on the custom fragment model. The user can define fragments' impact epoch, latitude longitude, velocity, mass and shape, as shown in Figure 24. In order to keep track of the origin of a fragment, the connection between the fragment and the previously defined component can be set by the user. By dragging and dropping a component from the *Satellite Model* (tree model as shown in Fig. 23) a new entry in the *Fragment List* can be created. In the *Connections* area, a list of identifiers will be shown, which trace back to the origin of the defined fragment.

## 5.4 Monte Carlo Mode

In DRAMA 3.0 the *Monte Carlo* mode was added. When activated the *Monte Carlo* sidebar entry is visible and can be used to vary input parameters of the simulation. The user can choose between five categories, which correspond to the variations in either the *Basic Settings*,



*the Satellite Model, Fragment Model, Metal Material or CFRP Material*. In the Basic Settings category, the user can define the *Sampling* method for e.g. the initial orbit or the beginning of the simulation. In the object and fragment categories the properties of the model can be altered. For example, the user can define a list of materials, which can be applied to an individual component. The re-entry simulation is then repeated for each material variation.

## 6 SUMMARY

To enable spacecraft builders to prove the compliance of their spacecraft with the corresponding regulations, ESA provides the DRAMA suite, including the SARA module, which is an object-oriented tool designed to analyse the re-entry of spacecraft and corresponding on-ground risk.

Within this activity, SARA was upgraded by implementing up-to-date methods and extending the functionality of the two existing submodules, SESAM and SERAM.

SESAM was rebuilt from scratch, providing a wide range of new functionalities such as connected-to and nested-in relations between modelled objects, as well as a wide variety of break-up and explosion triggers to end these relations during re-entry. The simulation uses pre-calculated aerodynamic and aero-thermodynamic coefficient databases for basic primitives and, through the implemented 'voxelator' module, shadowing effects between multiple connected objects are considered. The ablation algorithms can analyse the behaviour of metals and CFRP-like materials and NASA's EVOLVE 4.0 model has been implemented to cover the effect of explosion events.

SERAM was redesigned completely as well, supporting ground risk analysis for controlled and uncontrolled re-entries from LEO to HEO regions. Based on the re-entry type, the one-dimensional or two-dimensional casualty risk and fatality risk is determined from corresponding, up-to-date population data derived from the latest GWP and UNWPP models.

A Monte-Carlo wrapper module has been implemented to allow statistical analysis by four different types of parameter variation for the input to both modules, SESAM and SERAM. The different variation methods provide the ability to apply uncertainties for mission related parameters like the orbit state and re-entry trajectory and/or spacecraft related parameters for particular components or even materials implemented. Now, the footprint of surviving fragments can be analysed to determine the DRA and SRA values for controlled re-entries as requested by [1].

The upgraded DRAMA GUI provides additional functionality to ease the creation of spacecraft models,

also allowing to import/export materials or particular components for an improved compatibility and better re-usability between different projects. The user is supported by an extensive material and component database.

## 7 ACKNOWLEDGEMENT

The work performed for the *Upgrade of DRAMA's spacecraft entry survival analysis codes* is funded by ESA under Contract No. 4000115057/D/SR.

## 8 REFERENCES

1. ESSB-HB-U-002, "ESA Space Debris Mitigation Compliance Verification Guidelines", ESA, 2015/02/19.
2. Kuch, M., Entwicklung eines Modells für die ablativ Zerstörung von Kohlefaser-Epoxy Kompositen beim Wiedereintritt, Master thesis, TU Braunschweig, 2011.
3. Johnson, N. L. et al., "NASA's New Break up Model for Evolve 4", Adv. Space Research, Vol.29, no.9, pp 1377-1384, 2001; Pergamon Press.
4. P. M. Mehta, G. Blanco Arnao, D. Bonetti, E. Minisci and M. Vasile, "Computer Graphics for Space Debris", 6th International Conference on Astrodynamics Tools and Techniques (ICATT), Darmstadt, 2016.
5. D. Bonetti, C. Parigini, G. De Zaiacomo, I. Pontijas Fuentes, G. Blanco Arnao, D. Riley and M. Sánchez Nogales, "PETBOX: FLIGHT QUALIFIED TOOLS FOR ATMOSPHERIC FLIGHT", 6th International Conference on Astrodynamics Tools and Techniques (ICATT), Darmstadt, 2016.
6. D. Bonetti, I. Pontijas Fuentes, C. Parigini, G. Blanco Arnao, P. Palomo Pérez, F. Letterio, G. Vicario de Miguel, R. Travaglini, R. Sganga, S. Lemmens, T. Lips, R. Kanzler, "Upgrade of the Spacecraft Entry Survival Analysis Module (SESAM) of the ESA's Debris Risk Assessment and Mitigation Analysis (DRAMA) Tool", 67th International Astronautical Congress (IAC), Mexico, 2016.
7. C. Martin, J. Cheese, N. Sanchez Ortiz, K. Bunte, H. Klinkrad, T. Lips, B. Fritsche, G. Koppenwallner, "Debris Risk Assessment and Mitigation Analysis (DRAMA) Tool", Final Report of ESA/ESOC contract No. 16966/02/D/HK, QinetiQ/KI/Space/CR050073.
8. Armellin, R., "End-of-life disposal of high elliptical orbit missions: the case of integral", Advances in Space Research, 56 (3). pp. 479-493, 2015
9. Klinkrad, H., "Space Debris: Models and Risk Analysis", Springer, 2006

10. Center for International Earth Science Information Network - CIESIN - Columbia University, 2016, Documentation for the Gridded Population of the World, Version 4 (GPWv4). Palisades NY: NASA Socioeconomic Data and Applications Center (SEDAC), <http://dx.doi.org/10.7927/H4D50JX4>, Accessed 03 April 2017
11. Flegel, S., Gelhaus, J., Wiedemann, C., Oswald, M., Stabroth, S., Klinkrad, H., Krag, H., Vörsmann, P. (2009), *The MASTER-2009 Space Debris Environment Model*, in: Proceedings of the 5th European Conference on Space Debris, Darmstadt, Germany
12. Kebschull, C., Flegel, S., Gelhaus, J., Möckel, M., Braun, V., Radtke, J., Wiedemann C., Vörsmann, P., Sánchez-Ortíz, N., Krag, H. (2013), *The Software Architecture of the Upgraded ESA DRAMA Software Suite*, in: Proceedings of the 6<sup>th</sup> European Conference on Space Debris, Darmstadt, Germany
13. Schaaf, S.A. and Chambre, P.L. "Flow of rarefied Gases, High Speed Aerodynamics and Jet Propulsion" Princeton Univ. Press, Princeton, NJ, 1958
14. Regan, F. J., and AnandaKrishnan, S. M., "Dynamics of Atmospheric Re-Entry", AIAA Education Series, 1993
15. Zoby, E.V.; Moss, J.N.; Sutton, K. "Approximate convective-heating equations for hypersonic flows", 1981